# $S = \frac{1}{2}$ zigzag-chain structure and ferromagnetism of CdVO$_3$

Masashige Onoda and Noriaki Nishiguchi

Institute of Physics, University of Tsukuba, Tennodai, Tsukuba 305-8571, Japan

**Abstract.**    The crystal structure of the insulator CdVO$_3$ has been determined at 296 K by means of x-ray four-circle diffraction with residual factors of $R = 0.027$ and $R_w = 0.025$. The crystal data show an orthorhombic structure; space group $Pnma$, $a = 14.301(1)$ Å, $b = 3.598(1)$ Å, $c = 5.204(1)$ Å, and $Z = 4$. The isolated V zigzag chains with a nearest-neighbour V–V distance of 3.05 Å are formed along the $b$-axis by sharing edges and corners of VO$_5$ pyramids. The zigzag-chain unit and the VO$_5$ pyramid are almost identical to those of the two-dimensional $S = \frac{1}{2}$ system CaV$_2$O$_5$ which exhibits a simple dimer state with a gap of 660 K. The electronic states have been explored through magnetization and electron paramagnetic resonance measurements. CdVO$_3$ is an $S = \frac{1}{2}$ ferromagnet with a Curie temperature $T_C = 24$ K. The paramagnetic properties above 50 K are explained in terms of the ferromagnetic Heisenberg chain model in the classical limit, where $g = 1.96$ and the edge-sharing exchange coupling $J_e = -100.1(3)$ K, and the properties between 50 K and 30 K are considered as indicating a critical behaviour of the three-dimensional Heisenberg ferromagnet. This evidence is consistent with a previous model for the spin-gap formation of CaV$_2$O$_5$, in which it was postulated that the exchange coupling between the zigzag chains is rather larger than those within the zigzag chain.

M Supplementary data files are available from the article's abstract page in the online journal; see http://www.iop.org.

## 1. Introduction

The properties of various low-dimensional spin configurations have been explored intensively. The vanadium-based system which is a member of the compound series of transition metal ternary oxides and bronzes often exhibits spin-singlet ground states, such as bipolarons in $\beta$-Na$_{0.33}$V$_2$O$_5$ with a zigzag-chain structure [1] and trimers in LiVO$_2$ with a triangular lattice [2], which are accompanied by a lattice distortion due to electron–phonon interaction. The singlet state in (VO)$_2$P$_2$O$_7$ was once considered to be attributable to the properties of the two-leg spin ladder [3], but recently, a different interpretation in terms of an alternating-chain model has been given [4].

The CaV$_n$O$_{2n+1}$ insulator system with $n = 2$–4 consists of V$_n$O$_{2n+1}$ layers formed by sharing edges and corners of VO$_5$ pyramids, where Ca atoms are situated between the layers [5–7]. It has a two-dimensional $S = \frac{1}{2}$ configuration at the V$^{4+}$ (3d$^1$) site of the $[1/(n + 1)]$-depleted square lattice. CaV$_4$O$_9$ and CaV$_2$O$_5$ exhibit singlet ground states with energy gaps of $\Delta \simeq 110$ K [8] and 660 K [7, 9, 10], respectively. The mechanism of spin-gap formation for CaV$_4$O$_9$ may be explained from the viewpoint of the weakly coupled metaplaquette picture [8, 11], while the spin gap for CaV$_2$O$_5$ originates from the corner-sharing interchain dimer [10]. CaV$_3$O$_7$ does not exhibit a singlet state, but has a stripe-phase magnetic order [12,

13]. These results clearly indicate that corner-sharing superexchange interactions for the next-nearest-neighbour V–V path are very significant for determining the magnetic properties of this system.

Many vanadium oxides and bronzes have antiferromagnetic correlations, whose magnitude may be estimated roughly on the basis of structural chemistry [14, 15]. Recent theoretical work on the magnetic properties of $CaV_nO_{2n+1}$ postulates that all of the possible exchange couplings are antiferromagnetic. For example, considering an $S = \frac{1}{2}$ double-spin-chain system that seems to correspond to the V zigzag-chain unit of $CaV_2O_5$ has led to the proposal of various characteristic states for the antiferromagnetic coupling case, such as the Haldane, the dimer, the ladder, and the Majumdar–Ghosh models [16].

In order to establish the mechanism of spin-gap formation for $CaV_2O_5$, it is important to investigate the properties of the V zigzag-chain unit with V–O bond lengths and V–O–V bond angles similar to those of $CaV_2O_5$. The subject of this work is $CdVO_3$, for which neither crystal data nor structural models have been published [17, 18]. The magnetic susceptibility measurements at temperatures above 77 K indicate this compound to have ferromagnetic correlation [19]. This paper describes the precise crystal structure of $CdVO_3$ determined by means of x-ray four-circle diffraction, as well as the electronic states revealed through measurements of the magnetization and electron paramagnetic resonance (EPR). It will be shown that $CdVO_3$ has a completely isolated zigzag chain of V ions, and is one of the few vanadium compounds that are ferromagnetic. The zigzag-chain unit and the $VO_5$ pyramid of $CdVO_3$ are almost identical to those of $CaV_2O_5$, which may shed new light on the anomalous magnetic properties of $CaV_nO_{2n+1}$ and the related systems.

## 2. Crystal structure

Polycrystalline specimens of $CdVO_3$ were prepared by the solid-state reaction method as follows [19]. Mixtures of 4CdO (99.99% purity), $V_2O_5$ (99.99% purity), and $V_2O_3$ that was made according to the procedure described in reference [20] were ground and pressed into pellets. These were sealed in quartz tubes and then heated at 1073 K for 24 hours. The x-ray powder diffraction patterns measured at 296 K on a two-circle diffractometer with Cu K$\alpha$ radiation were very similar to those reported previously [17, 18], and agreed well with those calculated from the atomic parameters described below. The single crystals used in the structure analysis were obtained with an annealing temperature of 1173 K. Above this temperature, the specimens decomposed. $CdVO_3$ is an insulator.

The x-ray four-circle diffraction measurements were performed at 296 K on a Rigaku AFC-7R diffractometer (custom-made) with graphite-monochromated Mo K$\alpha$ radiation and a 18 kW rotating-anode generator. A crystal with dimensions of $0.02 \times 0.01 \times 0.09$ mm was mounted on a glass fibre. The intensity data for the structure analysis were collected over a maximum $2\theta$ range of $90°$ using the $\omega$–$2\theta$ scan technique. Of 1343 unique reflections, 725 reflections with $|F_o| \geqslant 3\sigma$, $F_o$ and $\sigma$ being an observed structure factor and its standard deviation, respectively, were used. Lorentz polarization, the absorption correction, and the extinction correction were applied, where the transmission factors were in the range 0.89–1.00. The internal consistency of the reflections was estimated on the basis of $F_o^2$ to be $R_{int} = 0.079$.

Through the systematic absences of reflections, a statistical analysis of the intensity distribution, and the successful solution and refinement of the structure, the crystal data were determined to be: orthorhombic with space group *Pnma* (No 62); $a = 14.301(1)$, $b = 3.598(1)$, $c = 5.204(1)$ Å, $V = 267.81(7)$ Å$^3$, $Z = 4$; $\mu$(Mo K$\alpha$) $= 11.18$ mm$^{-1}$; and $D_{cal} = 5.241$ Mg m$^{-3}$.

The structure was solved by direct methods [21], expanded using Fourier techniques, and refined by full-matrix least-squares calculations with anisotropic displacement parameters. The atomic scattering factors were taken from reference [22], and anomalous dispersion effects were included with the values given by reference [23]. The residual factors defined as

$$R = \sum (|F_o| - |F_c|)^2 \Big/ \sum |F_o|$$

and

$$R_w = \left[ \sum w(|F_o| - |F_c|)^2 \Big/ \sum w F_o^2 \right]^{1/2}$$

where $F_c$ is a calculated structure factor, are finally $R = 0.027$ and $R_w = 0.025$†. All of the calculations were performed using the teXsan crystallographic software package [24].

**Table 1.** Atomic coordinates, equivalent isotropic thermal parameters $B_{eq}$ ($\text{Å}^2$), and anisotropic displacement parameters $U_{ij}$ of $CdVO_3$ at 296 K, where $y = \frac{1}{4}$ and $U_{12} = U_{23} = 0$ for all of the atoms. $B_{eq}$ and $U_{ij}$ are defined by $B_{eq} = \frac{8}{3}\pi^2[U_{11}(aa^*)^2 + U_{22}(bb^*)^2 + U_{33}(cc^*)^2 + 2U_{12}aa^*bb^*\cos\gamma + 2U_{13}aa^*cc^*\cos\beta + 2U_{23}bb^*cc^*\cos\alpha]$, and the parameters are defined in the thermal factor form $T = \exp[-2\pi^2(a^{*2}U_{11}h^2 + b^{*2}U_{22}k^2 + c^{*2}U_{33}l^2 + 2a^*b^*U_{12}hk + 2a^*c^*U_{13}hl + 2b^*c^*U_{23}kl)]$.

| Atom | $x$ | $z$ | $B_{eq}$ | $U_{11}$ | $U_{22}$ | $U_{33}$ | $U_{13}$ |
|---|---|---|---|---|---|---|---|
| Cd | 0.318 42(3) | 0.138 32(8) | 0.912(5) | 0.0132(1) | 0.0105(1) | 0.0109(1) | −0.0025(1) |
| V | 0.080 58(6) | 0.082 6(2) | 0.65(1) | 0.0083(3) | 0.0081(3) | 0.0084(3) | −0.0005(2) |
| O1 | 0.109 6(3) | 0.393 0(8) | 1.31(7) | 0.019(2) | 0.020(2) | 0.011(2) | −0.001(1) |
| O2 | −0.057 9(3) | 0.042 1(8) | 0.91(6) | 0.012(1) | 0.008(1) | 0.014(2) | −0.001(1) |
| O3 | 0.194 1(2) | −0.106 4(7) | 0.77(5) | 0.007(1) | 0.011(1) | 0.011(1) | −0.001(1) |

**Table 2.** Selected interatomic distances (Å) of $CdVO_3$, where the translation codes are (i) $x, y, z$; (ii) $-x, -\frac{1}{2}+y, -z$; (iii) $-x, \frac{1}{2}+y, -z$; (iv) $\frac{1}{2}-x, -y, -\frac{1}{2}+z$; (v) $\frac{1}{2}-x, 1-y, -\frac{1}{2}+z$; (vi) $\frac{1}{2}+x, \frac{1}{2}-y, \frac{1}{2}-z$; (vii) $\frac{1}{2}-x, -y, \frac{1}{2}+z$; (viii) $\frac{1}{2}-x, 1-y, \frac{1}{2}+z$.

| VO5 pyramid | | Edges of pyramid | | Others | |
|---|---|---|---|---|---|
| V(i)–O1(i) | 1.668(4) | O1(i)–O2(i) | 3.012(5) | V(i)–V(ii, iii) | 3.048(1) |
| V(i)–O2(i) | 1.991(4) | O1(i)–O2(ii, iii) | 2.985(5) | V(i)–Cd(iv, v) | 3.2665(8) |
| V(i)–O2(ii, iii) | 1.940(2) | O1(i)–O3(i) | 2.866(6) | Cd(i)–O1(iv, v) | 2.434(3) |
| V(i)–O3(i) | 1.899(3) | O2(i)–O2(ii, iii) | 2.484(5) | Cd(i)–O2(vi) | 2.428(4) |
| — | | O3(i)–O2(ii, iii) | 2.673(4) | Cd(i)–O3(i) | 2.187(3) |
| — | | — | | Cd(i)–O3(vii, viii) | 2.244(2) |

The atomic coordinates, equivalent isotropic thermal parameters, and anisotropic displacement parameters are listed in table 1. Selected interatomic distances are listed in table 2. Figure 1(a) shows the crystal structure projected on the orthorhombic *ab*-plane, which is described by a linkage of $VO_5$ pyramids having apex oxygens in the direction of the *c*-axis with the normal displacement parameters. A clinographic view for the structure with the polyhedral scheme is shown in figure 1(b). The V zigzag chains extend along the *b*-axis by sharing edges and corners of the pyramids, where the nearest-neighbour V–V distance is 3.05 Å. The effective valence at the V site is estimated to be 4.0 (3d$^1$) on the basis of the bond-length–bond-strength relation [25]. The ground-state wavefunction of d$^1$ for the $VO_5$ pyramid

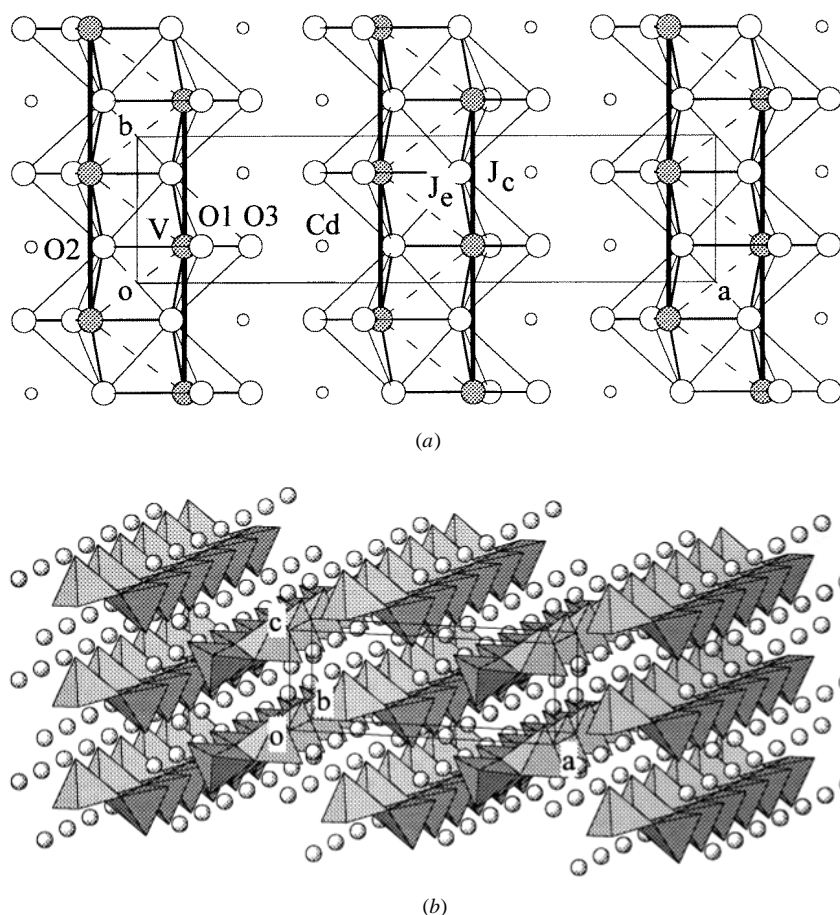† Supplementary data files are available from the article's abstract page in the online journal; see http://www.iop.org.

(*a*)



(*b*)

**Figure 1.** The crystal structure of CdVO$_3$ at 296 K: (*a*) the projection on the orthorhombic *ab*-plane, where the dashed lines and the thick ones show edge- and corner-sharing paths, respectively, responsible for the possible exchange couplings; and (*b*) a clinographic view with the polyhedral scheme, where the shaded spheres indicate Cd atoms.

is mainly composed of $-0.865d_{xy} + 0.503d_{yz}$, where $x \parallel a$ and $y \parallel b$, in terms of simple crystal-field analysis using the Hartree–Fock function for V$^{4+}$ [26]. Cd atoms are located between the chains and each surrounded octahedrally by six O atoms. Since the average Cd–O distance for the CdO$_6$ is 2.33 Å, the effective ionic radius of Cd$^{2+}$ is estimated to be about 0.95 Å, which is consistent with the value for six-coordinated Cd ions [27].

The edge- and corner-sharing paths in the zigzag chain responsible for the super-exchange interactions are shown by the dashed and the thick lines in figure 1(*a*), respectively. From table 2, the V–O–V angles for these paths are calculated to be 101.6(1)° and 136.1(2)°, respectively. The V zigzag-chain unit and the VO$_5$ pyramid revealed here are almost identical to those of CaV$_2$O$_5$, which are joined by sharing oxygen corners to form a two-dimensional layer, since the nearest-neighbour V–V distance and the next-nearest-neighbour one in the zigzag chain are 3.03 Å and 3.60 Å, respectively; and the V–O–V angles for the edge and corner linkages in the zigzag chain are 100.7° and 135.3°, respectively [7]. Therefore, exchange interactions in the zigzag chain are expected to be similar to those of CaV$_2$O$_5$. Further

discussion of the correlation between the crystal structure and the magnetic properties will be given in section 4.

## 3. Electronic states

Magnetizations with a field of up to 1 T for the polycrystalline specimens were measured by the Faraday method between 4.2 and 300 K. The magnetic susceptibility $\chi$ was deduced from the linear part of the magnetization–field ($M$–$H$) curve with a decreasing field.
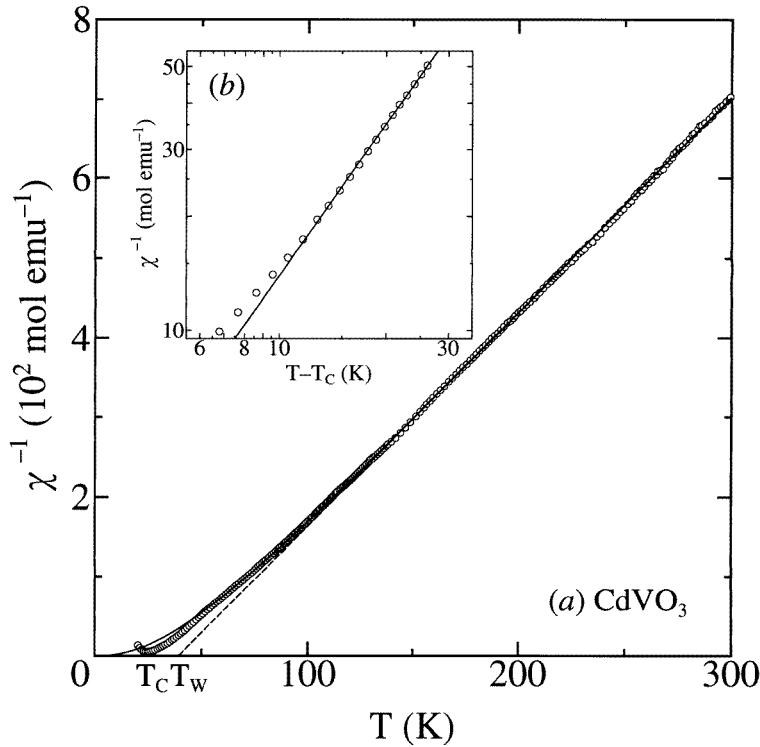


**Figure 2.** The temperature dependence of the magnetic susceptibility $\chi$ of CdVO$_3$: (*a*) $\chi^{-1}$ against $T$, where the full curve and the broken line indicate the calculated results in terms of the ferromagnetic Heisenberg chain model in the classical limit and a Curie–Weiss law, respectively, and $T_C$ and $T_W$ on the abscissa display the Curie and Weiss temperatures, respectively; and (*b*) $\log \chi^{-1}$ against $\log(T - T_C)$, where the full line shows a critical behaviour with an exponent of $\gamma = 1.33$.

The temperature dependence of $\chi^{-1}$ is shown by the open circles in figure 2(*a*). As temperature is lowered, $\chi^{-1}$ decreases with a ferromagnetic correlation, and has a minimum at 24 K which corresponds to the Curie temperature $T_C$ as described below. The behaviour above 50 K is explained in terms of the ferromagnetic Heisenberg chain model in the classical limit [28, 29]:

$$\chi = \frac{C}{T}\frac{1+u}{1-u} + \chi_0 \qquad \text{with } u = \coth\left(-\frac{3J}{4T}\right) + \frac{4T}{3J}$$

where $C$, $J$, and $\chi_0$ are, respectively, the Curie constant, the net exchange coupling [30], and the temperature-independent contributions from the Van Vleck orbital and diamagnetic susceptibilities. The full curve in figure 2(*a*) indicates the calculated result, with parameters

of $C = 0.3612(2)$ emu K mol$^{-1}$, $J = -100.1(3)$ K, and $\chi_0 = 0$. This Curie constant agrees well with the value estimated on the basis of the EPR $g$-factor which will be described later, and the $\chi_0$-value is close to those for $CaV_2O_5$ [7] and $MgV_2O_5$ [10]. The one-dimensional magnetic properties at high temperatures are consistent with the structural result. Here, the possible exchange interactions in the zigzag chain are $J_e$, through the edge-sharing path, and $J_c$, through the corner-sharing one, as shown in figure 1($a$). According to a qualitative rule for the exchange interactions [31, 32], it is possible for $J_e$ to become ferromagnetic when the effect due to direct overlap of 3d wavefunctions gives a minor contribution. The fact that the susceptibility data are well explained by just one parameter, $J$, over a wide temperature region with a reasonable Curie constant may indicate that even if $J_c$ is finite, it is significantly smaller than $|J_e|$. Therefore, $J$ corresponds to $J_e$.

For comparison, the result of Curie–Weiss analysis

$$\chi = \frac{C}{T + T_W} + \chi_0$$

where $T_W$ is Weiss temperature, for the behaviour above 120 K, is plotted as the broken line, where $C = 0.3716(4)$ emu K mol$^{-1}$, $T_W = -39.2(2)$ K, and $\chi_0 = 0$. When $|J_e| \gg J_c$, $J_e$ is about $-80$ K, which is 20% smaller than the value estimated above. This difference is of course attributed to that between the assumptions made for the models considered here. In the paramagnetic region between 50 K and 30 K, $\chi$ is considered as indicating a critical behaviour of the three-dimensional Heisenberg ferromagnet, $\chi \propto (T - T_C)^{-\gamma}$. Figure 2($b$) shows the comparison between experimental and calculated results, where the full line gives $\gamma = 1.33(1)$. This critical exponent is consistent with the value calculated from series expansions [33]. The deviation of the data from the calculated line between $T_C$ and 30 K is due to the so-called size effect as mentioned below.

Below 25 K, the remanent magnetization $\sigma$, defined as $M = \chi H + \sigma$, appears clearly. The $M$–$H$ curve at 5.1 K is shown in figure 3($b$), where the initial magnetization is displayed by the full circles, and a part of the hysteresis loop is indicated by the open circles and the full curve. On the basis of this result, the saturation magnetization is estimated to be $5.4 \times 10^3$ emu mol$^{-1}$, which corresponds to the value of the full moment for $S = \frac{1}{2}$ system with $g \simeq 2.0$, and the coercive force is about 9 mT. The temperature dependence of $\sigma$ extrapolated from the high-field side is shown in figure 3($a$) by the open circles. It is approximately expressed by the relation

$$\frac{\sigma}{\sigma_0} = \tanh\left(\frac{\sigma T_C}{\sigma_0 T}\right)$$

with $\sigma_0 = 5.4 \times 10^3$ emu mol$^{-1}$ and $T_C = 24$ K as shown by the full curve. Here, a slight disagreement between the experimental and calculated results around $T_C$ is attributed to a short-range-order effect.

EPR measurements for the polycrystalline specimens were performed at 9.2 GHz using a JEOL spectrometer at temperatures between 14 and 300 K. The signal is single Lorentzian at temperatures above 30 K. The extracted spin susceptibility is comparable with the static susceptibility, which is consistent with the result that the static susceptibility comes from the V spins. The peak-to-peak linewidth of the absorption derivative at 300 K is 32 mT, which decreases monotonically with the decrease of temperature, and is 7 mT at 30 K. Below this temperature, the signal is asymmetric due to the presence in the specimen of inhomogeneous, effective local magnetic fields [34]. The $g$-factor is nearly temperature independent, $g = 1.961$, which corresponds to the values for Heisenberg magnets with similar $VO_5$ pyramids and the $d_{xy}$-type ground-state wavefunction [10].

Thus, the electronic states of $CdVO_3$ at high and low temperatures are characterized as $S = \frac{1}{2}$ Heisenberg ferromagnets in one and three dimensions, respectively.
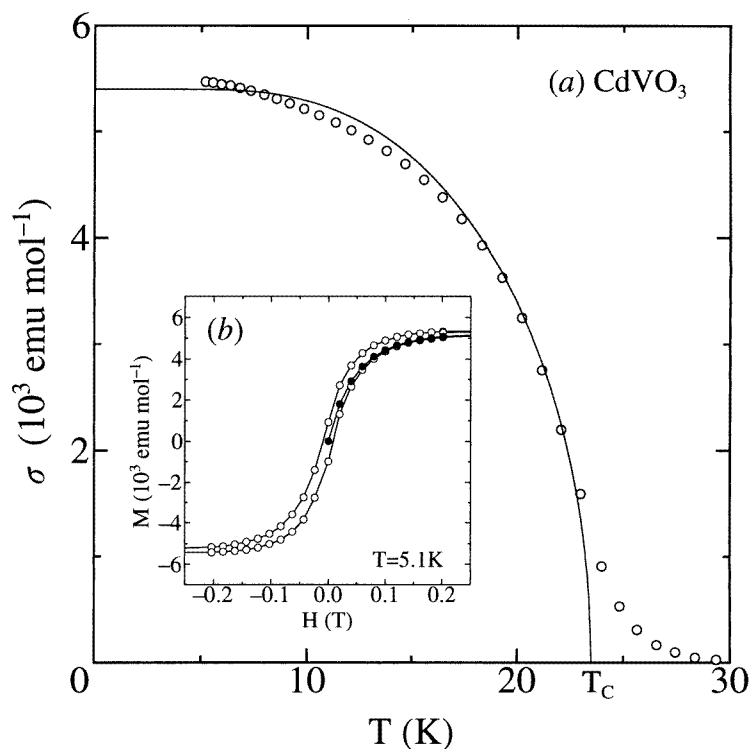
**Figure 3.** (*a*) The temperature dependence of the remanent magnetization $\sigma$ of CdVO$_3$, where the full curve indicates the result based on the Brillouin function with $S = \frac{1}{2}$, and (*b*) the field dependence of the magnetization *M* at 5.1 K, where the full circles indicate the initial magnetization, and the open circles and the full curve indicate a part of the hysteresis loop for the region $-1$ T $\leqslant H \leqslant 1$ T.

## 4. Discussion and conclusions

The crystal structure and electronic states of CdVO$_3$ have been explored by x-ray four-circle diffraction and through measurements of the magnetization and EPR.

CdVO$_3$ has a one-dimensional V zigzag chain formed along the *b*-axis by sharing edges and corners of V$^{4+}$O$_5$ pyramids and it is an $S = \frac{1}{2}$ ferromagnet with $T_C = 24$ K. To the best of our knowledge, this compound is the first example of an ionic ferromagnetic vanadium compound with a half-filled state. The paramagnetic properties at temperatures above 50 K are explained in terms of the ferromagnetic Heisenberg chain model in the classical limit with $g = 1.96$ and the edge-sharing exchange coupling $J_e = -100$ K, and the properties between 50 K and 30 K are interpreted as indicating a critical behaviour of the three-dimensional Heisenberg ferromagnet. Quantum spin effects in one dimension at temperatures well below the exchange coupling energy [29] do not appear due to the three-dimensional coupling between the zigzag chains.

The V zigzag chain and the VO$_5$ pyramid revealed here are almost identical to those in the two-dimensional layer of CaV$_2$O$_5$ which exhibits an isolated dimer state with a gap of 660 K. A previous model proposed by one of the authors for the spin-gap formation of CaV$_2$O$_5$ has postulated that the exchange coupling within the zigzag chains is rather smaller than that for interchain bonds, if all of the couplings are antiferromagnetic [10]. For MgV$_2$O$_5$ with a two-

dimensional layer similar to that of $CaV_2O_5$, the V zigzag chain and the $VO_5$ pyramid are a little different from those discussed here. In this case, the exchange coupling between the zigzag chains is reduced significantly, so the ratio of exchange couplings within the zigzag chain to the interchain coupling should increase relatively. This will lead to a significant reduction of the magnitude of the spin gap if it is finite [10, 15]. The present result indicates that for the zigzag chain of $CdVO_3$, only the edge-sharing exchange coupling is effective and ferromagnetic, and the corner-sharing coupling is not relevant to magnetic properties. This is consistent with the dimer model for $CaV_2O_5$. In order to understand these properties quantitatively, an accurate estimation of the kinetic and potential exchange couplings on the basis of the detailed crystal structure is necessary.

$\gamma$-$LiV_2O_5$ also has V zigzag chains which consist of $V^{4+}O_5$ pyramids, but these are connected by $V^{5+}O_5$ pyramids [35, 36]. The magnetic properties of this compound appear to be explained in terms of the Bonner–Fisher model for an $S = \frac{1}{2}$ antiferromagnetic Heisenberg chain system [37], although the reported $g$-factor, 1.8, is rather smaller than our EPR value, 1.94 [38]. The significant difference of magnetic properties for the V zigzag-chain systems should be attributed to that of the spin-density distributions of the oxygen ions.


## Acknowledgment

## References

[1] Onoda M and Nagasawa H 1987 *Phys. Status Solidi* b **141** 507 and references therein
[2] Onoda M and Inabe T 1993 *J. Phys. Soc. Japan* **62** 2216 and references therein
[3] See, for example, Dagotto E and Rice T M 1996 *Science* **271** 618 and references therein
[4] Garrett A W, Nagler S E, Tennant D A, Sales B C and Barnes T 1997 *Phys. Rev. Lett.* **79** 745
[5] Bouloux J-C and Galy J 1973 *Acta Crystallogr.* B **29** 1335
[6] Bouloux J-C and Galy J 1973 *Acta Crystallogr.* B **29** 269
[7] Onoda M and Nishiguchi N 1996 *J. Solid State Chem.* **127** 359
[8] Kodama K, Harashina H, Sasaki H, Kobayashi Y, Kasai M, Taniguchi S, Yasui Y, Sato M, Kakurai K, Mori T and Nishi M 1997 *J. Phys. Soc. Japan* **66** 793 and references therein
[9] Iwase H, Isobe M, Ueda Y and Yasuoka H 1996 *J. Phys. Soc. Japan* **65** 2397
   The magnitude of spin gap estimated from the Knight shifts and the spin–lattice relaxation times of the $^{51}V$ nuclei in terms of the isolated dimer model is about 600 K.
[10] Onoda M and Ohyama A 1998 *J. Phys.: Condens. Matter* **10** 1229
   For this work, a table of observed and calculated structure factors is available in the on-line version. This reference suggests that $MgV_2O_5$ remains paramagnetic due to the frustration effects or has magnetic order due to the three-dimensional correlation, where the exchange coupling for interchain bonds is reduced significantly as compared with that of $CaV_2O_5$. On the other hand, reference [15] postulates the existence of a small spin gap on the assumption that all of the possible exchange couplings of $MgV_2O_5$ are comparable with those of $CaV_2O_5$.
[11] Fukumoto Y and Oguchi A 1998 *J. Phys. Soc. Japan* **67** 2205 and references therein
[12] Harashina H, Kodama K, Shamoto S, Taniguchi S, Nishikawa T, Sato M, Kakurai K and Nishi M 1996 *J. Phys. Soc. Japan* **65** 1570
[13] Kontani H, Zhitomirsky M E and Ueda K 1996 *J. Phys. Soc. Japan* **65** 1566
[14] Pickett W E 1997 *Phys. Rev. Lett.* **79** 1746
[15] Millet P, Satto C, Bonvoisin J, Normand B, Penc K, Albrecht M and Mila F 1998 *Phys. Rev.* B **57** 5005
[16] See, for example, Nakamura T, Takada S, Okamoto K and Kurosawa N 1997 *J. Phys.: Condens. Matter* **9** 6401
[17] Galy J and Bouloux J-C 1967 *C. R. Acad. Sci., Paris* **264** 388
[18] Reuter B and Müller K 1969 *Z. Anorg. Allg. Chem.* **368** 174
[19] Chamberland B L and Danielson P S 1974 *J. Solid State Chem.* **10** 249
[20] Onoda M, Ohta H and Nagasawa H 1991 *Solid State Commun.* **79** 281

[21] Debaerdemaeker T, Germain G, Main P, Refaat L S, Tate C and Woolfson M M 1988 *MULTAN88: Computer Programs for the Automatic Solution of Crystal Structures from X-Ray Diffraction Data* (University of York)
[22] Cromer D T and Waber J T 1974 *International Tables for X-Ray Crystallography* vol 4, ed J A Ibers and W C Hamilton (Birmingham: Kynoch) section 2
[23] Creagh D C and McAuley W J 1992 *International Tables for Crystallography* vol C, ed A J C Wilson (Boston, MA: Kluwer Academic)
[24] teXsan 1992 *Crystal Structure Analysis Package* (The Woodlands, TX: Molecular Structure Corporation)
[25] Zachariasen W H 1978 *J. Less-Common Met.* **62** 1
[26] Freeman A J and Watson R E 1965 *Magnetism* part A, vol 2, ed G T Rado and H Suhl (New York: Academic)
[27] Shannon R D 1976 *Acta Crystallogr.* A **32** 751
[28] Fisher M E 1964 *Am. J. Phys.* **32** 343
[29] For a review, see Auerbach A 1994 *Interacting Electrons and Quantum Magnetism* (New York: Springer) ch 18
[30] The Heisenberg Hamiltonian is defined as $H = \Sigma_{\langle i, j \rangle} J S_i S_j$, $S_i$ being the spin operator at site $i$.
[31] See, for example, Goodenough J B 1963 *Magnetism and the Chemical Bond* (New York: Interscience) ch 3
[32] Huang N L and Orbach R 1968 *J. Appl. Phys.* **39** 426
[33] See, for example, Ma S-K 1976 *Modern Theory of Critical Phenomena* (London: Benjamin) ch 2
[34] Schlömann E 1969 *Phys. Rev.* **182** 632
[35] Anderson D N and Willett R D 1971 *Acta Crystallogr.* B **27** 1476
[36] Onoda M 1997 unpublished results
Analysis for the V–O bond length on the basis of the detailed atomic parameters determined by means of x-ray four-circle diffraction, where $R = 0.033$ and $R_w = 0.024$ for 924 independent reflections ($|F_o| \geqslant 3\sigma$), indicates the valence distributions of $V^{4.2+}$ and $V^{5+}$ at the V1 and V2 sites, respectively.
[37] Isobe M and Ueda Y 1996 *J. Phys. Soc. Japan* **65** 3142
[38] Onoda M 1984 unpublished data